http://dx.doi.org/10.5516/NET.07.2014.706

IRRADIATION PERFORMANCE OF U-Mo MONOLITHIC FUEL

M.K. MEYER[1*], J. GAN[1], J.F. JUE[1], D.D. KEISER[1], E. PEREZ[1], A. ROBINSON[1], D.M. WACHS[1], N. WOOLSTENHULME[1], G.L. HOFMAN[2], and Y.S. KIM[2]
[1]Idaho National Laboratory
2525 Fremont Avenue, Idaho Falls, ID USA – 83415
[2]Argonne National Laboratory
9700 S. Cass Avenue, Lemont, IL USA – 60439
[*]Corresponding author. E-mail : mitchell.meyer@inl.gov

Received March 22, 2014

High-performance research reactors require fuel that operates at high specific power to high fission density, but at relatively low temperatures. Research reactor fuels are designed for efficient heat rejection, and are composed of assemblies of thin-plates clad in aluminum alloy. The development of low-enriched fuels to replace high-enriched fuels for these reactors requires a substantially increased uranium density in the fuel to offset the decrease in enrichment. Very few fuel phases have been identified that have the required combination of very-high uranium density and stable fuel behavior at high burnup. U-Mo alloys represent the best known tradeoff in these properties. Testing of aluminum matrix U-Mo aluminum matrix dispersion fuel revealed a pattern of breakaway swelling behavior at intermediate burnup, related to the formation of a molybdenum stabilized high aluminum intermetallic phase that forms during irradiation. In the case of monolithic fuel, this issue was addressed by eliminating, as much as possible, the interfacial area between U-Mo and aluminum. Based on scoping irradiation test data, a fuel plate system composed of solid U-10Mo fuel meat, a zirconium diffusion barrier, and Al6061 cladding was selected for development. Developmental testing of this fuel system indicates that it meets core criteria for fuel qualification, including stable and predictable swelling behavior, mechanical integrity to high burnup, and geometric stability. In addition, the fuel exhibits robust behavior during power-cooling mismatch events under irradiation at high power.

KEYWORDS : U-Mo, Monolithic Fuel, Research Reactor, Dispersion, Irradiation Testing, Low-enriched Uranium

1. INTRODUCTION

High-performance research reactors require fuel that operates at high specific power to high fission density, but at relatively low temperatures. Research reactor fuels are designed for efficient heat rejection, and so are largely composed of assemblies of thin-plates that use aluminum alloy cladding. Inside the cladding, the fuel core (often called the fuel meat) is typically composed of fuel particles dispersed in an aluminum matrix. Theses fuels are referred to as 'dispersion' fuels (Fig. 1).

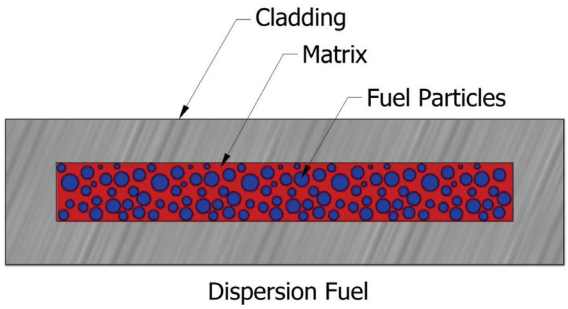

Fig. 1. Schematic Dispersion Fuel Cross-section (Not to Scale).

The development of LEU (low-enriched uranium) fuels for high-performance research reactors is an important nonproliferation objective.[1] The replacement of HEU (High-Enriched Uranium) research reactor fuel with LEU fuel results in the avoidance of several hundred kilograms of HEU commerce annually. The development of these LEU fuels requires increased uranium density in the fuel to offset the decrease in enrichment. A suitable high-uranium-density fuel phase must therefore be identified, developed as part of a fuel system, and qualified for service. Conversion of reactors that currently use HEU must occur without significant impact to reactor mission performance, safety, or operating cost.

Research reactor fuels operate at low peak fuel temperatures but are required to meet fuel performance requirements to high burnup. Typical peak fuel centerline temperatures are less than 250°C, with fuel in most reactors operating at significantly lower temperatures. Required peak fuel phase fission densities are typically in the range of $3x10^{21}$ to $6x10^{21}$ f/cm^3. In a few cases, peak fuel phase fission density requirements exceed $7x10^{21}$ f/cm^3, approaching depletion of all initial ^{235}U atoms. There are few fuel

phases that have the combination of very-high uranium density and stable fuel behavior to the high burnup required for fuels suitable for conversion of these high power density reactors. The two classes of fuels that approach or meet uranium density requirements are gamma stable uranium alloys with 10 wt.% or less alloy content and the class of U_6Me ordered i ntermetallic phases (Me = transition metal). Of these two fuels, U_6Fe and U_6Mn[2,3] have been evaluated through irradiation testing, and have demonstrated undesirable breakaway swelling behavior at fuel phase fission densities on the order of $3x10^{21}$ f/cm^3, far short of the requirements for LEU conversion fuels. It is likely that other U_6Me compounds will exhibit the same behavior.

2. PRIOR U-MO FUEL DEVELOPMENT EFFORTS

A variety of reactor types have utilized U-Mo metallic alloy fuels in the past, because of the combination of high uranium density and material properties. Beginning in 1960, U-Mo alloys were used in pulsed reactors Godiva IV at Los Alamos, VIPER in England, the Health Physics Research Reactor at Oak Ridge, Super Kukla at the Nevada Test Site, the Fast Burst Reactor (FBR) at White Sands, the Army Pulsed Radiation Facility (Aberdeen, MD), and the Sandia Pulsed Reactor II. Two used α-phase U-1.2 wt% Mo. The other five used γ-phase U-10wt% Mo. The higher alloy content (10 wt%) fuel eliminated anisotropy in properties and increased material strength. Fuels were pulsed to temperatures as high as 600°C, but because of the short irradiation times, the effects of fuel burnup were minimal.[4]

Another early application was for the Organic Moderated Reactor (OMR) at the Piqua Nuclear Generating Station in Ohio (the site was built and operated between 1963 and 1966 as a demonstration by the Atomic Energy Commission). The fuel element was built using cast U-3.5Mo-0.1 Al cylindrical plates, with aluminum fins to enhance cooling efficiency.[5] This and a flat-plate fuel design were both considered and tested to prove a life expectancy of 5000MWd/MTU peak burnup at a specified peak-fuel centerline temperature of 454°C.[6] The plant operated for about three years, but was shut down because of flow blockage and control-rod sticking caused by irradiation effects on the organic coolant.

The Dounreay Fast Reactor (criticality, 1959; full power, 1963) used a number of metal-fuel- based designs. These included U- 9.1 wt% Mo and then U-7 wt% Mo clad in niobium. The 9.1-wt%-Mo fuel swelled slightly less than the 7 wt%-Mo alloy, but the more highly alloyed fuel cracked more and, with an increase in the number of experiments being placed in DFR, there was a need for higher uranium density; thus the U-9.1Mo alloy was abandoned. All of these fuels were of annular design, clad inside and out. Some of the designs, when operated in certain areas of the reactor, achieved reasonably high burnups (4-9 at%) without breach of the cladding before accommodation of swelling was designed into fast-reactor fuels.[7]

The EFFBR (Enrico Fermi Fast Breeder Reactor) was the first commercial fast reactor. A 200 MWt (60 MWe) three-loop design, it was approved by the AEC in 1955 and operation at 100 MWt began in July 1966. The fuel was U-10Mo, sodium-bonded to Zircaloy cladding. The EFFBR fuel prototypes were tested thoroughly before use to demonstrate that the U-10Mo alloy could perform to reactor design specifications;[8] the primary concern was to ensure that the fuel would maintain the γ-phase during operation. A series of experiments mapped the fission rate and temperature dependence of γ–phase stability. U-Mo has also been studied for potential use in light water reactors in Russia and the United States. A number of U-alloy fuels have been tested, including U-9Mo in a zirconium alloy matrix and in a magnesium matrix.[9,10]

The Hallam Nuclear Power Facility (HNPF), a graphite-moderated sodium-cooled reactor of 240 MWt, operated from 1962 to 1964 in Nebraska. HNPF fuel consisted of U-10Mo cylindrical rods sodium bonded to stainless steel cladding. Fuel development and testing was carried out by Atomics International in Idaho at the Materials Test Reactor (MTR).[11]

3. URANIUM ALLOY FUEL BEHAVIOR

In the operating temperature range of interest to research and test reactor applications (below ~250°C), unalloyed uranium exists in the anisotropic (orthorhombic) α-U phase. α-U exhibits dimensional instability under irradiation in the form of anisotropic growth and swelling. This anisotropic dimensional change in individual grains (in a polycrystalline sample) results in mismatched strains at the microstructural level. The stress developed due to these mismatched strains can be released by tearing or cavitation at grain boundaries. γ-U has a bcc (body centered cubic) crystal structure and exhibits isotropic swelling behavior, which eliminates this issue. The γ-U phase is stable in the temperature range of 776°C to the melting point of uranium (1135°C). Alloying with molybdenum (and certain other elements) results in a sluggish transformation from γ-phase to the equilibrium phases on cooling.

Extensive studies and characterization of U-Mo alloys have investigated the transformation kinetics[12,13,14,15,16,17,18,19] of the U-Mo system in the uranium-rich region of the phase diagram. The decomposition rate of the γ-phase on cooling is a function of the Mo concentration in the alloy. Early studies by Pfeil,[20] Saller et al.,[21,22,23] Ivanov et al.[24] and Dwight et al.[25] focused on the $\gamma\text{-U} \rightarrow (\alpha\text{-U} + \gamma' (U_2Mo))$ decomposition. Howlett et al.,[26] Repas et al.[27] and Goldstein et al.[28] developed TTT (Time-Temperature-Transformation) diagrams for U-Mo alloys, ranging from 2.5 to 14 wt.% Mo. Certain ternary element additions, including Pt and Ru, in combination with Mo can further increase the γ-stabilizing effect. Re, Pd, and Os are other potential candidates.[29,30,31] This increase in gamma stability comes at

no cost in terms of density, however it does not appear to be necessary for ensuring stable irradiation behavior in U-Mo fuels, because of the occurrence of irradiation-induced phase reversion, discussed below. The class of U-Nb-Zr alloys also exhibits sluggish γ-phase decomposition behavior.[32,33,34] Time-temperature-transformation plots for U-Mo based alloys and a lower-density U-Nb-Zr alloy are shown in Figure 2.

The relationship between γ stability and uranium density for U-Nb, U-Nb-Zr, and U-Mo alloys is plotted in Figure 3. Because both high density and the largest region of γ-phase metastability are desirable, U-Mo alloys represent the best tradeoff in these properties for LEU research reactor fuels.

During irradiation, provided sufficient alloy content and fission rate, U-Mo alloys will revert from the equilibrium

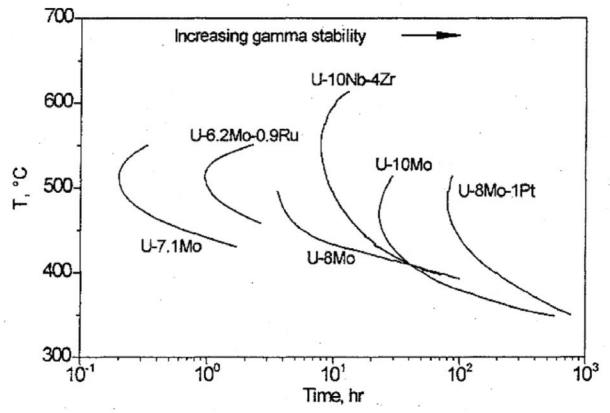

Fig. 2. The Relationship between Alloy Content, Time, and Start of Decomposition from the γ-U Phase for Alloys of Interest for Research Reactor Fuel.

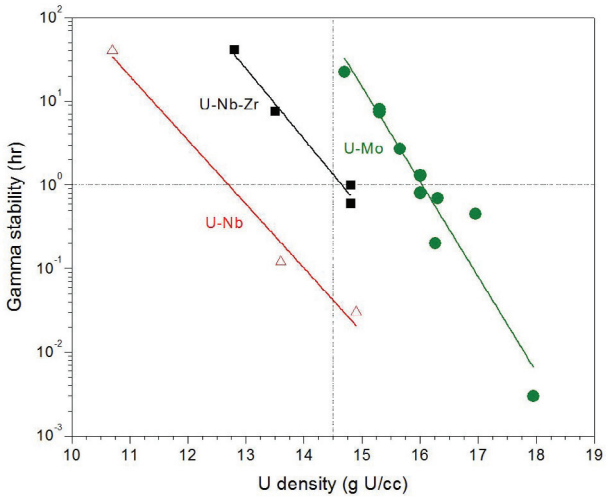

Fig. 3. Tradeoff between Uranium Density and Gamma Stability (Indicated by the Nose of the Time-temperature-transformation Diagram) for U-Nb, U-Nb-Zr, and U-Mo Alloys.

α-U + U_2Mo (γ′) phases (or intermediate phases formed during decomposition of the γ(U-Mo)phase) back to the metastable γ(U-Mo phase).[35,36] This behavior is hypothesized to be the result of fission spikes that induce disordering of the γ′ (U_2Mo) phase and mixing at the atomic level to produce a homogeneous composition of uranium and molybdenum in the γ phase. The required fission rate for phase reversion decreases with temperature below the nose of the time-temperature-transformation curve, consistent with the tendency for longer times prior to decomposition of the metastable phase at lower temperatures.

Ten fuel alloys were selected for initial irradiation testing on the basis of the stability of the γ-phase, uranium density, neutron absorption cross-section, stability against reaction with the aluminum matrix, and stability under irradiation. The test matrix from the initial (RERTR-1 and RERTR-2) experiments is provided in Table 1. Test fuel plates in the RERTR-1 test train were irradiated to a burnup of approximately 40% to provide an initial indication of performance. The RERTR-2 test extended irradiation to approximately 70% burnup. Both tests were conducted at moderate fission power levels and fuel loadings of approximately 4.8 g-U/cm^3 to reduce the risk of experiment failure, since behavior of these fuels under high-burnup conditions had not previously been tested.

The behavior of fuel alloys was consistent with expectations based on γ-phase stability.[37] A series of optical micrographs that illustrates the differences in behavior in U-10Mo, U-6Mo, U-4Mo, and U-5Nb-3Zr alloys after irradiation are shown in Figures 4 and 5. In general, alloys that contained more than 6 wt.% Mo exhibited acceptable irradiation behavior under these conditions, exhibiting a small and uniform fission gas bubble population that indicates stable swelling. There was minimal reaction of the fuel with the aluminum matrix. U-4Mo (Fig. 4 (c)) formed large fission gas bubbles that are beginning to interlink, indicative of the first stages of breakaway swelling, at approximately 70% ^{235}U burnup. U-5Nb-3Zr (Fig. 5) exhibited behavior similar to U-4Mo, but beginning at a burnup of approximately 40% ^{235}U. On this basis, U-Mo alloys were selected as the fuel phase for development of very-high-density dispersion fuels.

Table 1. Initial Test Matrix to Determine the Feasibility of U Alloy Fuels

U-Mo alloys	U-Nb-Zr alloys	Ternary alloys	Other fuels
U-10Mo	U-9Nb-3Zr	U-6Mo-1Pt	U_2Mo
U-8Mo	U-6Nb-4Zr	U-6Mo-0.6Ru	U_3Si_2
U-6Mo	U-5Nb-3Zr	U-10Mo-0.05Sn	
U-4Mo			

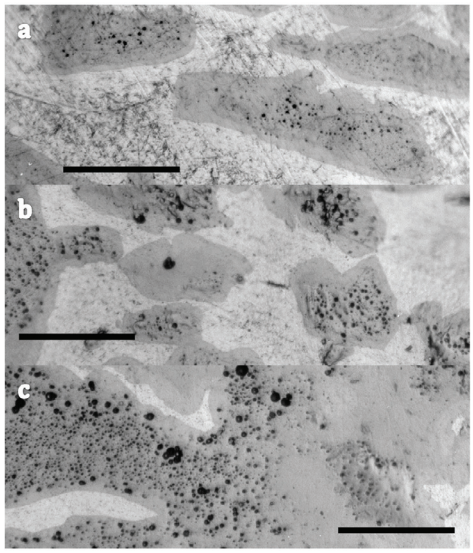

Fig. 4. Comparison of the Irradiation Behavior of U-Mo Alloys at Approximately 70% ^{235}U Burnup: (a) U-10Mo, (b) U-6Mo, (c) U-4Mo. Scale Bar Indicates 50 Micrometers.

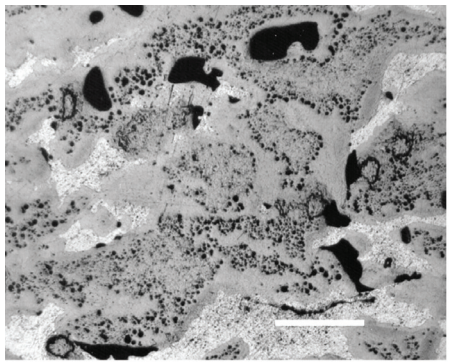

Fig. 5. Microstructure of Irradiated U-5Nb-3Zr Alloy Irradiated to Approximately 41% ^{235}U Burnup. Scale Bar Indicates 50 Micrometers.

4. U-MO DISPERSION AND MONOLITHIC FUELS

Subsequent higher power, high-burnup testing of aluminum matrix U-Mo dispersion fuel revealed a pattern of breakaway swelling behavior at intermediate burnup. Breakaway swelling is defined by a span of stable fuel behavior, followed by a rapid or unpredictable transition to high swelling behavior. Post-irradiation examination of the U-Mo dispersion fuel microstructure revealed that the high swelling was related to the formation of a ternary [(U-Mo)Al_X] aluminide phase that had formed by reaction of the U-Mo fuel particles with the aluminum fuel matrix during irradiation (see, for example).[38,39,40] Reaction between the U-Mo and aluminum occurs during irradiation at high power, resulting in the formation of the medium gray (U-Mo)Al_X phase. This phase releases fission gas at the boundary between the interaction phase and the aluminum matrix.

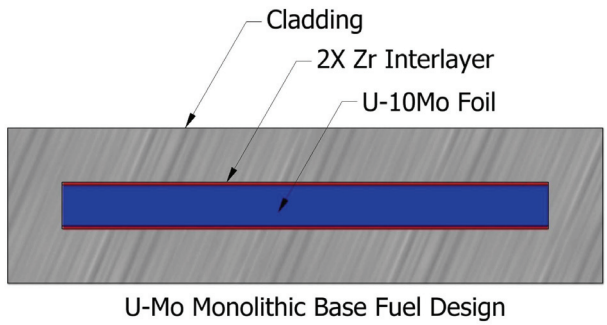

Fig. 6. Depiction of Monolithic Fuel Cross-section (Not to Scale).

These gas bubbles tend to agglomerate into gas pockets, which have the combined effect of weakening the fuel meat in the through-thickness direction while exerting internal gas pressure. The result is a mechanical failure of the fuel meat, resulting in fuel plate delamination and a large plate thickness increase.

Microstructural examination of failed fuel plates shows uniformly that the U-Mo fuel particles have behaved well, in contrast to the (U-Mo)Al_X reaction product formed in reactor. Eliminating the (U-Mo)Al_X related failure mode involves eliminating or stabilizing the (U-Mo)Al_X phase. At least four methods have been experimentally evaluated. These include: (1) Coating the U-Mo particles to prevent interaction with the matrix[41], (2) modifying the solid state chemistry of the aluminum/uranium/molybdenum system,[42] (3) substituting the aluminum matrix in the fuel core with an alternative matrix material (magnesium)[43] or (4) eliminating the matrix entirely. Elimination of the matrix, (4) results in a laminated structure in which a U-Mo foil is encapsulated by and bonded to the aluminum alloy cladding. This fuel type is referred to as 'monolithic U-Mo fuel' (as opposed to a dispersion of U-Mo particles in aluminum). Figure 6 provides a depiction of a cross-section of the monolithic fuel design.

5. MONOLITHIC FUEL FABRICATION

Any new nuclear fuel first requires the development of conceptual fabrication technology to prepare samples for irradiation testing. The first monolithic fuel mini-plates were produced using hot rolling processes similar to those used for dispersion fuel plates. These plates were then irradiated in the Advanced Test Reactor (ATR) at Idaho National Laboratory (INL) to evaluate the behavior of the fuel design. Based on the generally good irradiation behavior observed,[44] an effort to further develop monolithic fuel technology began.

A variety of fabrication techniques were evaluated[45,46,47,48] and, in some cases, carried through irradiation testing. Monolithic fuel is fabricated, in general by (1) alloying and

casting, (2) foil rolling, 3) bonding of the cladding, and (4) finishing and inspection for quality assurance. Fabrication processes for monolithic U-Mo fuel are continuously being refined; the following paragraphs provide an outline of the process.[49]

Alloying is typically performed through vacuum induction melting (VIM) or arc melting of uranium and molybdenum metals at a temperature of ~1300-1500°C. The molten alloy is typically cast into a coated graphite book mold. The casting is surface machined into a 'coupon' of the appropriate size for reduction into a foil though hot and cold rolling.

Foil fabrication involves reducing the thickness of a cast alloy coupon to the desired fuel foil thickness while simultaneously bonding the Zr barrier layer to the surface of the U-Mo. Hot rolling operations are conducted with the alloy temporarily encapsulated in a steel rolling can. This allows the material to be heated to 650°C in air without oxidizing the fuel alloy and the Zr. After decanning, the resulting U-10Mo fuel foil, bonded to two thin (0.025 mm) layers of zirconium, sandwiched between two sheets of aluminum and placed in a steel can for HIP (Hot Isostatic Press) processing. The HIP process is typically conducted at a temperature of 560°C for a time of 90 minutes or longer. The HIP can is cut open; the bonded plates are removed, and the plates are finished to final dimensions and inspected.

6. MICROSTRUCTURE AND INTERFACES

The microstructure of U-Mo foil depends on feedstock impurity content, the starting condition of the fuel coupon, and the rolling schedule as discussed in [50]. The size and morphology of the grains that comprise the bulk U-10Mo-alloy foil microstructure depend on the thermo-mechanical treatments that are used during fuel-plate fabrication. Molybdenum depleted and enriched regions in the as-cast microstructure resulting from solidification from the melt become elongated features during rolling, and bands of differing Mo concentration can be observed in the final foil. These bands can be several to tens of microns thick and can exhibit a variation of 2-3 wt% Mo throughout the foil in an as-fabricated fuel plate. Decomposition of the original gamma (U,Mo) phase results in a lamellar structure comprised of α-U and γ'-phase. These lamellar structures can also manifest themselves as bands within the foil microstructure.

A key feature that defines the irradiation performance of monolithic fuel is the interface between the fuel meat and the cladding. Good bonding between the fuel meat and cladding throughout irradiation ensures good thermal conductivity and that fuel-plate 'pillowing' during irradiation does not occur that may result in cooling channel restriction or fission product release. Although the fuel/clad interface temperature is low in monolithic fuel, fission gas bubble formation and interlinkage at the U-Mo/Al interface has been observed[51] in the aluminum-rich U-MoAl_x reaction product that has formed at the U-Mo/Al interface. Because the mechanical stability of the fuel-to-cladding interface is critical to maintaining acceptable fuel performance, two methods were developed to mitigate this potential failure mode. Early testing performed on dispersion fuel-meat designs demonstrated that the addition of small amounts of silicon to the aluminum matrix could be used to suppress the growth of the interaction layer and appears to stabilize the interaction layer that forms.[52,53] Based on these observations, fuel designs were developed and tested to evaluate performance of a silicon-enriched interface. Testing of this design revealed that fuel-to-cladding bonding was weak after irradiation.

The second design approach was based on minimizing interaction between the U-Mo fuel foil and the cladding through introduction of a diffusion barrier. A barrier thickness of 25 μm was selected to exceed the maximum fission fragment recoil range (~9 μm in Zr) and to allow for inherent thickness variability in the manufacturing process. Zirconium, niobium, and molybdenum were considered as barrier materials. Based on the performance of early irradiation tests with zircaloy clad U-Mo mini-plates[54] and coated particle testing[55] coupled with the successful application of Zr to the fuel foil using a hot co-rolling process, the Zr-barrier-based design was selected for qualification.

The U-Mo/Zr interface contains multiple phases that develop during the interdiffusion that occurs between U-10Mo and Zr during the co-rolling and HIP processes. U-Mo-Zr ternary phase diagrams have been determined by Ivanov and Bagrov for isothermal temperature of 500, 575, 600, 625, 650, 675, 700, 750 and 1000°C.[56,57] The 575°C and 650°C diagrams can be used to predict the phases and diffusion paths that may be observed in a diffusion zone that develops at the U-10Mo/Zr interface during co-rolling and HIPing. Systematic diffusion-couple experiments have been performed at 600, 650, 700, 800, 900, and 1000°C using U-10Mo and high-purity Zr.[58] Significant inter-diffusion was observed for all the couples annealed at 700°C or higher. Negligible interdiffusion was observed at 600°C. The Arrhenius temperature dependence of growth rate for the interdiffusion zone found in the diffusion couples, U-10Mo vs. Zr, is presented in Figure 7. The measured growth rate at 800, 900, and 1000°C and calculated values at 500, 600, and 700°C are shown.

Perez et al. used transmission electron microscopy (TEM) to investigate the phases at the U- 10Mo/Zr interface in an as-fabricated DU-10Mo monolithic fuel plate[59] with Zr diffusion barrier fabricated as part of the AFIP-3 experiment. A schematic diagram representing the main phases observed at the U-10Mo/Zr interface for the characterized sample is presented in Figure 8. Phases observed near the U-10Mo interface with the Zr diffusion barrier include: UZr_2, γ-UZr, Zr solid solution and Mo_2Zr phases. Small amounts of α-U were also observed in the Mo depleted zone that forms.

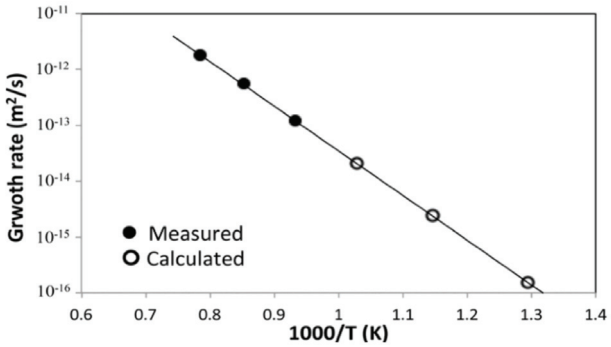

Fig. 7. Arrhenius Temperature Dependence of Growth Rate for Interdiffusion Zone Found in the Diffusion Couples, U-10Mo vs. Zr. The Measured Growth Rate at 800, 900, and 1000°C and Calculated Values at 500, 600, and 700°C are Represented by Solid and Empty Circles, Respectively.

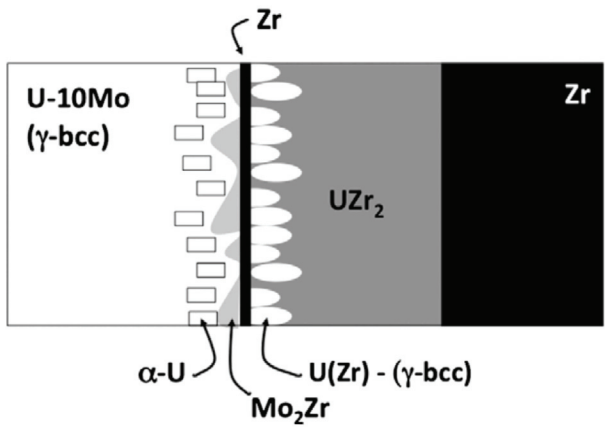

Fig. 8. A Schematic Representation of Microstructure at the Interface between a U-10 wt.% Mo Fuel Plate and Zr Diffusion Barrier.

The Zr/Al-6061 cladding interface must also be well-bonded and stable. This multi-phase zone develops during HIP processing. Ten different binary Al-Zr intermetallic compounds exist, eight of which are low-temperature phases,[60] however, only two phases have been experimentally observed at temperatures below the melting point of aluminum (660°C). The binary Al-Zr system has not been exhaustively investigated in the α-Zr region. In 1964, Kidson and Miller noted the formation of only one intermetallic, $ZrAl_3$, in the temperature range of 553-640°C during interdiffusion experiments. In 2004, Laik et al. published results in which they used EPMA to identify, not only the formation of $ZrAl_3$ between 565-625°C, but also the formation of Zr_2Al_3 at temperatures above 600°C.[61] No further investigation into this discrepancy has been conducted.

Results of recent diffusion experiments performed between Zr and AA6061 cladding are reported in [62]. In the AA6061 vs. Zr couples annealed at and above 560˚C, a thick layer of $(Al,Si)_3Zr$ phase with low Si content was observed to develop, while thinner layers of Al_5SiZr_2 and

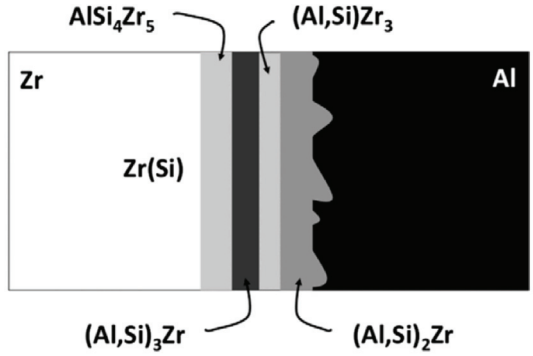

Fig. 9. Schematic Representation of Microstructure at the Interface between the Zr Diffusion Barrier and Al-6061.

$(Al,Si)_2Zr$ phases developed at the AA6061/$(Al,Si)_3Zr$ and $(Al,Si)_3Zr$/Zr interfaces, respectively. Negligible diffusional interaction between AA6061 vs. Zr was observed at 450˚C. These results indicate that Zr is an attractive option for use as a diffusion barrier with proper selection of temperature for thermo-mechanical processing and thermal annealing.

TEM examination has also been conducted on as-fabricated U-Mo monolithic fuel plates to determine the phases present at the Zr/Al-6061 interface during production.[59] A schematic diagram representing the main phases observed at the Zr/Al-6061 interface for the characterized sample is presented in Figure 9.

7. IRRADIATION BEHAVIOR

LEU-Mo monolithic fuel plates must exhibit mechanical integrity, geometric stability and stable and predictable swelling behavior during irradiation to prevent coolant flow blockage and/or release of fission products. The key phenomena that can impact the dimensional stability and robustness of a fuel plate during irradiation are fuel swelling, transformation of radiation-stable phases into unstable phases, radiation-enhanced diffusion between dissimilar materials resulting in the formation of unstable phases, creep of materials, and mechanical-property degradation.

Fuel swelling is driven by solid and gaseous fission products. Solid fission product swelling is caused by the increase in the volume of solid fission products relative to the volume of uranium atoms. It is dependent on burnup in a linear manner, and independent of temperature and fuel alloy content[63] for a given uranium density.

The gas-driven fuel swelling rate is low at fission densities less than 3×10^{27} fissions/m^3. Initially, fission gas in U-Mo precipitates in a fcc (face-centered-cubic) superlattice of nano-size bubbles that are registered on the underlying bcc U-Mo crystal lattice.[64,65] Gas bubbles are approximately 3 nm in diameter and are arrayed on a uniform face-centered cubic lattice, with a lattice parameter of approximately 12 nm (Figure 10). Although gas remains

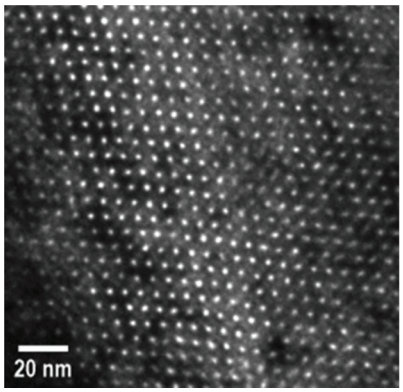

Fig. 10. Nano-scale Fission Gas Bubbles in U-Mo at $3x10^{21}$ fissions/cm^3.

contained in the fission gas bubble lattice in regions of the microstructure at fission densities upwards of $4x10^{27}/m^3$, at a fission density between 2.5×10^{27} and 3.5×10^{27} fissions/m^3, gas-driven swelling increases in importance. This transition is attributed to grain refinement or 'recrystallization', which provides additional defect sites for fission gas bubble formation.[66,67] As grain refinement progresses at higher burnup, more grain surfaces become available for bubble formation and growth. Some of the nano-bubbles appear to contribute to the formation of larger bubbles in the intergranular regions. The nano bubble supperlattice near the grain boundaries is gradually destroyed as nano bubbles near boundaries coalesce to form micron-scale bubbles in the intragranular regions. At higher fission densities, localized regions of the crystalline, γ-(U,Mo) phase can become amorphous, as observed using TEM.

The combination of solid fission product swelling and gas-driven swelling results in the recommended fuel swelling correlations[68] provided in equations (2) and (3):

Equation (1): $\Delta V/Vo = 5.0 f_D$
for $f_D \leq 3x10^{27}$ fissions/m^3

Equation (2): $\Delta V/Vo = 15 + 6.3(f_D\text{-}3) + 0.33(f_D\text{-}3)^2$
for $f_D > 3x10^{27}$ fissions/m^3

Where f_D Fission density is in 10^{27} fissions/m^3. The correlations show mild non-linearity; the fuel-swelling rate increases slightly as fission density increases caused by the increasingly important role of micron-scale fission-gas bubbles. It is important to note that no indications of break-away swelling have been observed in U-Mo fuel irradiated to fission densities higher than achievable for LEU fuel.

An example of the evolution in microstructure is provided in Figure 11, along with corresponding swelling data provided in Figure 12, measured by immersion density. These data are from the RERTR-12 test, where fifty-six monolithic fuel test plates where irradiated under a range of conditions applicable to U.S. high performance research reactors. At fission densities in the range of $2.2x10^{27}$ to $4.0x10^{27}$ f/m^3, little microstructural change is apparent

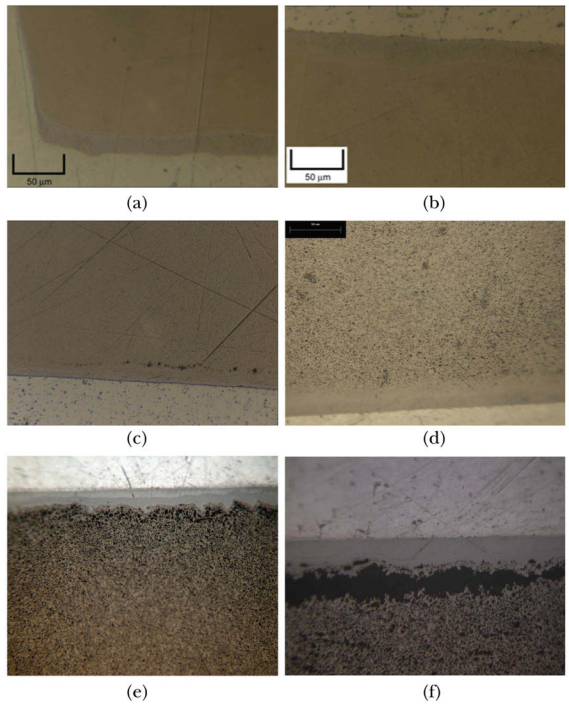

Fig. 11. Evolution of U-10Mo Monolithic Fuel Microstructure as a Function of Local Fission Density (10^{27} f/m^3). (a) 2.2, (b) 4.0, (c) 6.2, (d) 7.2, (e) 8.4, (f) 9.5.

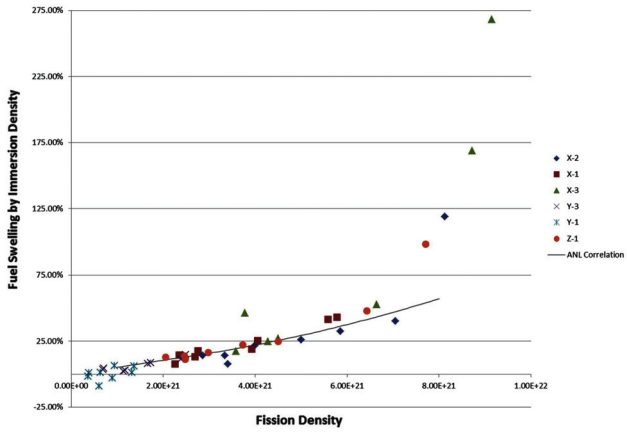

Fig. 12. Plot of U-Mo Swelling Measured using Immersion Density vs. Average Fission Density. The Solid Line Depicts the Swelling Correlation of Equations (1) and (2). Note that Plates Exhibit Failure in Regions of Highest Fission Density, Typically > 20% Higher than Average Fission Density.

using optical metallography. Microstructural changes can be observed using SEM and TEM.[69,70] As fission density increases from $4.0x10^{27}$ f/m^3 to $6.2x10^{27}$ f/m^3, grain refinement occurs and formation of micron-scale porosity is visible in some regions near the U-Mo/Zr interface. At a local fission density of $7.2x10^{27}$ f/m^3, grain refinement has occurred throughout the majority of the microstructure,

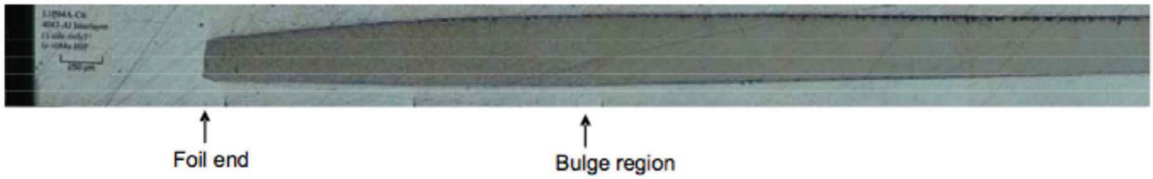

Fig. 13. Optical Micrograph of Metallographic Section of the Edge Region of a Monolithic Fuel Plate. The Thick Region of the Plate Interior to the Constrained end of the Foil forms because of Irradiation-enhanced Creep.

resulting in the formation of microporosity throughout the U-Mo fuel meat; note also the lack of porosity at the U-Mo/Zr interface in this region. A fission density of 7.8×10^{27} f/cm^3 represents complete burnup of all the initial ^{235}U atoms in LEU-10Mo fuel; fission density exceeding complete LEU burnup was achieved by using uranium of higher enrichment. Growth of micron-sized bubbles in the bulk regions of the fuel continues as fission increases to 8.4×10^{27} f/m^3 (11(e)). Delamination of the fuel near the U-10Mo/Zr interface occurs at a local fission density of 9.5×10^{27} f/m^3, resulting in a fuel plate volume increase. Note that plate failures occur in the regions of the fuel plates with the highest fission density, typically >20% above the average fission density. Peaks in fission density are caused by power peaking at the ends and edges of fuel plates in this test configuration. The swelling and failure behavior is consistent for all plates in this test series, showing delamination at the same threshold value in the region of highest fission density, indicating that the fuel system exhibits predictable behavior and maintains mechanical integrity to burnup levels achievable with LEU.

Irradiation enhanced creep is a second key phenomenon that makes the monolithic fuel system viable. Fuel foils are constrained from swelling in the plane of the fuel plate by the cladding rails, and examination of irradiated fuel plates shows that little or no dimensional change is measured in this plane. An increase in the volume (swelling) of a thin plate constrained at all four edges and capable of plastic deformation results in a thickness increase, as shown in the metallographic cross section of Figure 13. Virtually all swelling is manifested in the fuel-meat thickness.

The maximum foil thickness increase occurs away from the edge of the plate, and is larger than can be explained by fission-product swelling, as plotted in Figure 14. The formation of this thick region can be explained by irradiation enhanced creep of the fuel,[71] driven by the stress that builds up at the rail constraint caused by fission-product swelling. Swelling at the plate edges is lower than expected, due to the constraint of the plate rail. Fuel moves inward by irradiation-enhanced creep to form the thick region approximately 3 mm from the edge of the foil. The recommended relationship for irradiation enhanced creep is:

$$\varepsilon_F = A\sigma f_R$$

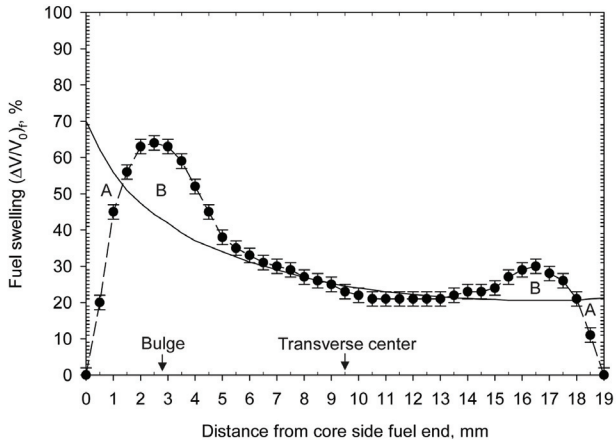

Fig. 14. Comparison of Expected (Solid Line) vs. Measured (Points and Dashed Line) Plate Swelling Across the Width of a Miniplate.

where $A = 500 \times 10^{-25}$ cm^3/MPa, σ is stress in MPa, and f_R is the average fission rate in the fuel in fissions/m^3-s. It should be noted that there is considerable uncertainty in the value of the creep rate constant (A).

8. DEMONSTRATION OF PERFORMANCE

The AFIP-6MkII test demonstrated the mechanical integrity, geometric stability, and predictable behavior of full-size U-Mo monolithic fuel to very high powers and high fission densities. This test operated at a peak beginning-of-life heat flux of 5,700 kW/m^2 (corresponding to a peak volumetric power of 35 MW/m^3) to a peak fission density of 4.3×10^{27} f/m^3. Postirradiation ultrasonic and visual images are shown in Figure 15. No indications of inadequate performance in the form of blistering, warping, or high swelling were detected using ultrasonic testing and visual examination.

Geometric stability of fuel plates against bowing or deflection during irradiation that might result in coolant channel restrictions was demonstrated by measuring the changes in coolant channel gap geometry of a four plate model demonstration fuel element as a function of burnup. The fuel element design for this test is depicted in Figure 16. Channel gap widths were measured using a specially designed ultrasonic probe prior to irradiation, between

Fig. 15. Postirradiation Visual Examination (Top) and Ultrasonic Examination (Bottom) of AFIP-6MkII Fuel After Irradiation to $4.3x10^{27}$ f/m^3 at a Peak Power of 35 MW/m^3. No Indications of Delamination, Blistering, Warping, or High Swelling were Observed.

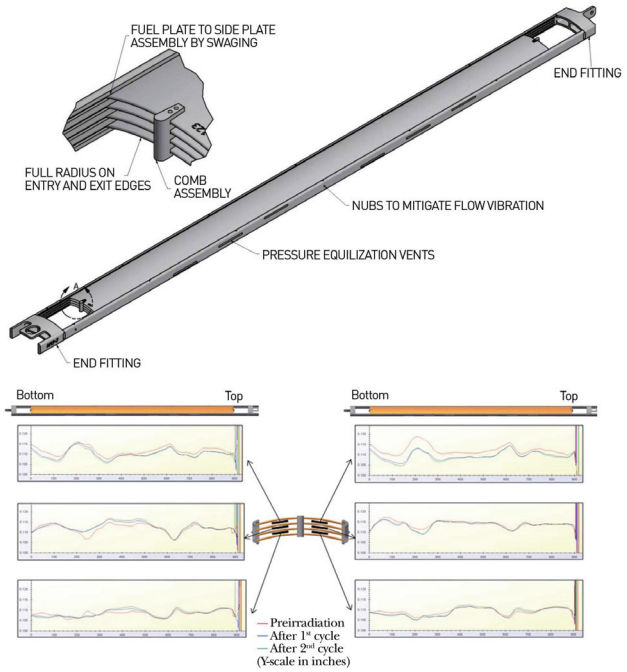

Fig. 16. (a) Drawing of Fuel Element Configuration used to Test Geometric Stability. (b) Channel Gap Width Measurement Traces Prior to Irradiation and after the First and Second Cycles of Irradiation. The Y-axis Indicates Channel Gap Spacing in Inches, the X-axis Indicates Position along the Length of the Water Channel (Dimensionless).

irradiation cycles, and after irradiation, and indicate a maximum deflection of less than 0.1 mm after irradiation to a peak burnup of $3.3x10^{27}$ f/m^3.

9. OFF-NORMAL BEHAVIOR

The response of the fuel during irradiation at conditions well in excess of normal operating conditions[72] is an important feature demonstrated by the AFIP-6 irradiation test. This test was performed as a 'bounding case' test meant to envelope the key operating conditions (power and burnup) for the highest power U-Mo monolithic LEU fuel designs. The experiment had nearly completed the first of two planned irradiation cycles when minor fission product releases to the ATR primary coolant system were identified, resulting in termination of the test at a peak fission density of $3.5x10^{27}$ f/m^3. Subsequent detailed thermal hydraulic analysis of the experiment indicated that the combination of the high operating power and test vehicle configuration led to high operating temperatures for the fuel plates. This elevated temperature led to accelerated surface corrosion which resulted in a thick, low thermal conductivity oxide layer that resulted high fuel temperatures.

Surface heat fluxes for this test as a function of time are shown in Figure 17, and peak at approximately 500 W/cm^2 at beginning of life. Fuel thermal conditions are calculated by coupling plate power conditions with oxide thickness measurements. Eddy current measurements of oxide thickness were indicated a peak oxide thickness of 240 μm, more than an order of magnitude thicker than typically measured. The fuel meat temperature profile is very sensitive to the thermal conductivity of the oxide layer. The relatively thin layer of boehmite on the surface has a thermal conductivity value of approximately 0.0225 W/cm/K but beneath this layer is a relatively thick, complex layer aluminum oxide, aluminum, and porosity. The thermal conductivity of this material was estimated by treating it as a two-phase system where the remaining aluminum is dispersed in an oxide matrix using a modified Hashin and Shtrikman correlation.[73] Based on these estimates, it is likely that the fuel plates operated at a peak fuel meat temperature approaching 500°C (Figure 18). The fuel plate was designed to operate below 225°C (see Fig. 18).

ATR stack gas activity monitoring indicated that approximately five discrete releases occurred over the last 11 days of operation, as shown in Figure 19. Visual examination of the fuel plate surface showed variable surface oxide thickness from the plate top to bottom. At the top of the fuel zone a region of typical oxide conditions was observed. This region was followed by a region that covered most of the fuel plate's fuel zone and consisted of a dark, rough textured layer that covered the hottest regions of the fuel plate, indicating that a thick oxide layer had formed. In-canal ultrasonic examination was performed to further characterize the surface morphology and internal features of both fuel plates. The examination confirmed the presence of delaminated regions of the fuel plate. The black spots shown on Figure 20 are the delaminated areas. Ultrasonic measurement of the local plate thickness in the areas where delaminations occurred indicated the

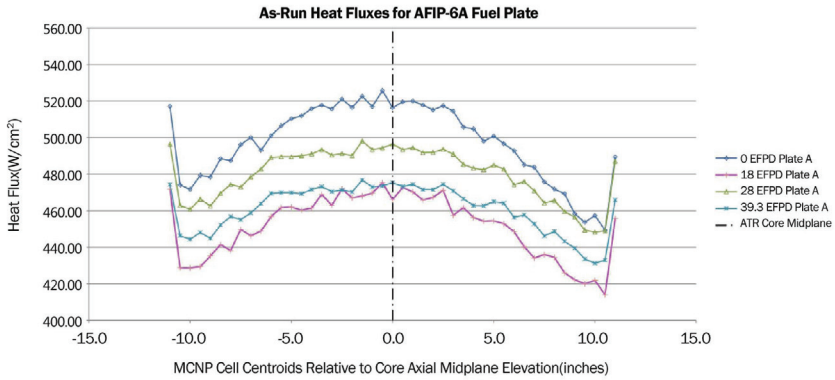

Fig. 17. Calculated AFIP-6 Fuel Plate Surface Heat Flux at Beginning of Life and 18, 28, and 39.3 Days of Irradiation.

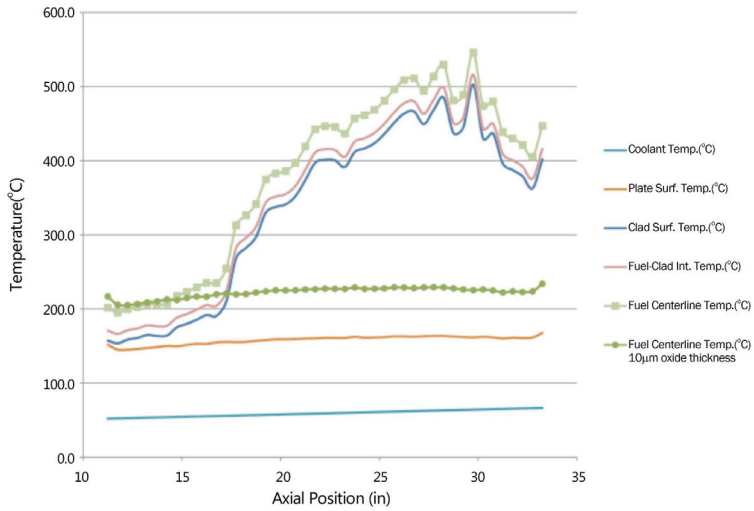

Fig. 18. Calculated Fuel Temperatures as a Function of Axial Location on the Fuel Plate.

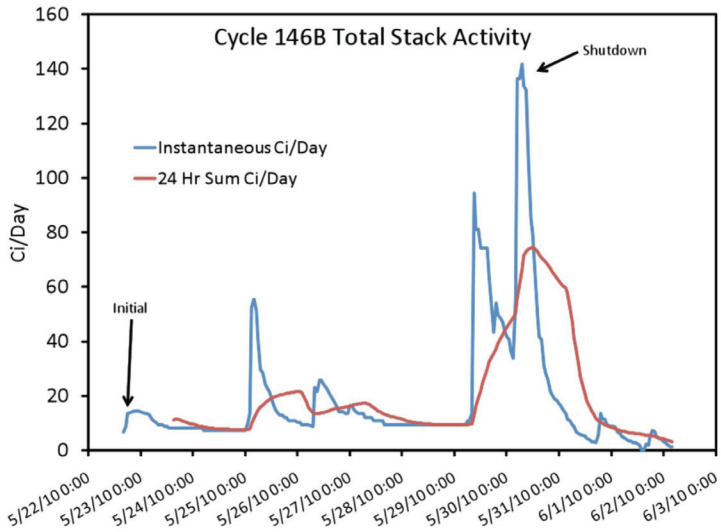

Fig. 19. Stack Gas Activity Measured as a Result of Releases from the AFIP-6 Experiment, Consistent with Release from Blisters that Resulted from Fuel Plate Overheating.

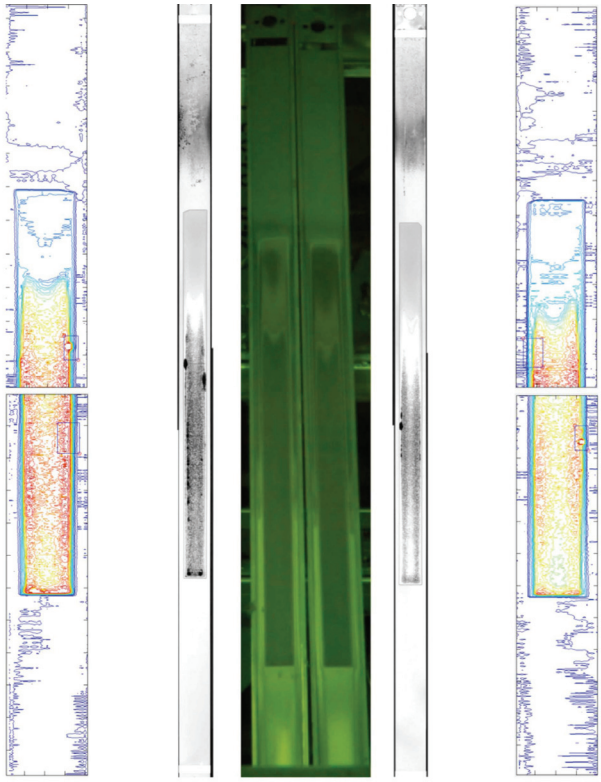

Fig. 20. Ultrasonic Thickness Scans (a & e) Indicate Raised Portions on the AFIP-6 Fuel Plates in Areas where Delamination is Detected (b & d). Dark Coloration in Underwater Photographs (c) Indicates a Thick Oxide Layer.

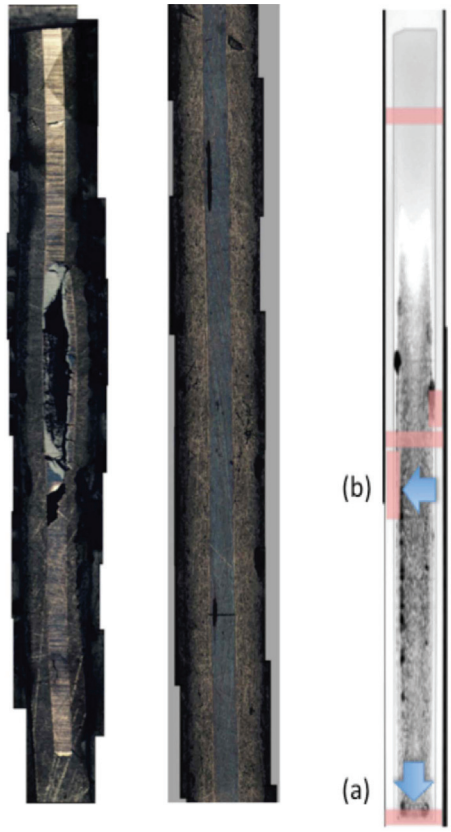

Fig. 21. Metallographic Images of Blister Cross-sections (a) Transverse Blisters at Lower end of Fuel Plate and (b) Longitudinal Blisters in Center Region of Plate.

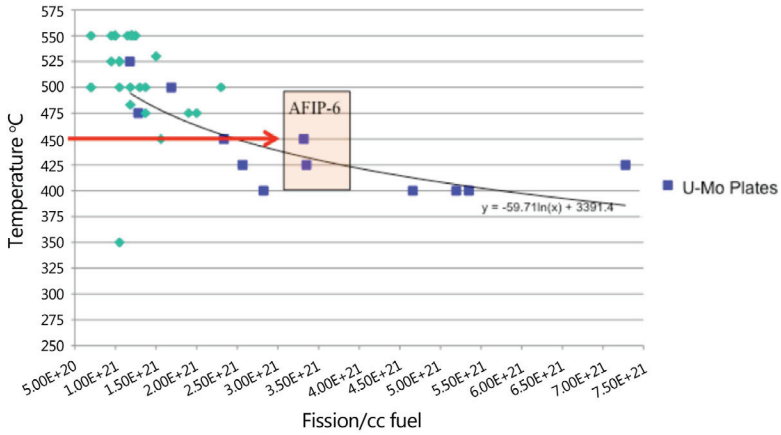

Fig. 22. The Estimated Range of in-reactor Blister Temperatures for AFIP-6 Plotted with Data from Out-of-pile Blister Tests of U-Mo (Squares) and U_3O_8 (Diamonds).

presence of increased thickness in these areas, consistent with fuel blistering. Metallographic images (Figure 21) confirm that blisters formed in the U-Mo fuel meat, and that the fuel/cladding interface did not delaminate. These blisters were observed to form in the peak power regions of the plates (e.g. along the edges of the fuel at core centerline and at the plates lower end) where the temperature and fission density were at a maximum. Fission product releases observed during irradiation were likely caused by these thermally induced blisters. The morphology of the pores observed during metallography also support this gas release mechanism. These in-reactor blister threshold temperatures are consistent with those measured out-of-pile for other research reactor fuel types, as shown in Figure 22.

10. SUMMARY

Based on scoping irradiation test data, a low-enriched uranium monolithic fuel plate system composed of solid U-10Mo fuel meat, a zirconium diffusion barrier, and Al6061 cladding was selected for development as a low-enriched uranium research reactor fuel. Developmental testing of this fuel system indicates that it meets core criteria required to continue with fuel qualification. These criteria include stable and predictable swelling behavior, demonstrated mechanical integrity to high burnup, and geometric stability of the plates to the fission density required for research reactor fuel element designs for specific reactors. In addition, the fuel exhibits robust behavior during reduced flow events when under irradiation at high power. Fabrication technology development is underway to allow scale up for commercial production. Fabrication process variants will be tested in the MiniPlate-1 irradiation beginning in 2017. A specific process variant will be selected for qualification through a series of tests that further demonstrate that the fuel is qualified for use in research and test reactors.

ACKNOWLEDGEMENT

This work was supported by the U.S. Department of Energy, Office of Nuclear Materials Threat Reduction (NA-212), National Nuclear Security Administration, under DOE–NE Idaho Operations Office Contract DE-AC07-05ID14517. Accordingly, the U.S. Government retains a non-exclusive, royalty-free license to publish or reproduce the published form of this contribution, or allow others to do so, for U.S. Government purposes. This information was prepared as an account of work sponsored by an agency of the U.S. Government. Neither the U.S. Government nor any agency thereof, nor any of their employees, makes any warranty, express or implied, or assumes any legal liability or responsibility for the accuracy, completeness, or usefulness of any information, apparatus, product, or process disclosed, or represents that its use would not infringe privately owned rights. References herein to any specific commercial product, process, or service by trade name, trademark, manufacturer, or otherwise, does not necessarily constitute or imply its endorsement, recommendation, or favoring by the U.S. Government or any agency thereof. The views and opinions of the authors expressed herein do not necessarily state or reflect those of the U.S. Government or any agency thereof.

REFERENCES

[1] J. L. Snelgrove, G. L. Hofman, M. K. Meyer, C. L. Trybus, T. C. Weincek, "Development of Very-High Density Low Enriched Uranium Fuels," *Nucl. Eng. Des*., 178, pp 119-126 (1997).

[2] M. K. Meyer, T. C. Wiencek, S. L. Hayes, and G. L. Hofman, "Irradiation Behavior of U_6Mn-Al Dispersion Fuel Elements," *J. Nucl. Mater*., 278, pp. 358-363 (2000).

[3] G. L. Hofman, R. F. Domogala, and G. L. Copeland, "Irradiation Behavior of Low-Enriched U_6Fe-Al Dispersion Fuel Elements," *J. Nucl. Mater*., 150 pp. 238-243 (1987).

[4] J. A. Horak, J. A. Reuscher and D. J. Sasmor, "Operating Experience with Uranium-Molybdenum Fuel in Pulsed Reactors," Symposium on Materials Performance in Operating Nuclear Systems, Ames, Iowa, August (1973).

[5] E. B. Baumeister, and J. D. Wilde, "Selection of the Piqua OMR Fuel Element," report NAA-SR-4239, Atomics International (1960).

[6] M. H. Binstock, "Fuel Element Development for Piqua OMR," report NAA-SR-5119, Atomics International (1960).

[7] S. A. Cottrell, E Edmonds, P. Higginson, and W. Oldfield, "*Development and Performance of Dounreay Fast Reactor Metal Fuel*," Proceedings of the Third U. N. International Conference on the Peaceful Uses of Atomic Energy, Geneva, A/Conf 28/P/150 (1964).

[8] A. A. Shoudy, W. E. McHugh and M. A. Silliman, "The Effect of Irradiation Temperature and Fission Rate on the Radiation Stability of Uranium-10 wt% Molybdenum Alloy," Radiation Damage in Reactor Materials, International Atomic Energy Agency, Vienna, pp. 133-162 (1963).

[9] A. Savchenko, A. Vatulin, I Konovalov, A. Morozov, V. Sorokin, S. Maranchak, "Fuel of Novel generation for PWR and as Alternative to MOX fuel," *Energy Conversion and Management*. 51, pp. 1826-1833 (2010).

[10] "Development status of metallic, dispersion and non-oxide advanced and alternative fuels for power and research reactors," International Atomic Energy Agency, IAEA-TECDOC-1374 (2003).

[11] R. M. Willard and A. R. Schmitt, "Irradiation Swelling, Phase Reversion and Intergranular Cracking of U-10wt%Mo Fuel Alloy", Atomics International report NAA-SR-8956 (1964).

[12] H. A. Saller, F. A. Rough, and A. A. Bauer, "Transformation Kinetics of Uranium-Molybdenum Alloys," United States Atomic Energy Commission report BMI-957 (1954).

[13] R. F. Hills, B. R. Butcher, J. A. Heywood, "A study of the effect of cooling rate on the decomposition of the γ-phase in uranium-low molybdenum alloys," *J. Less Common Metals*, 3:2, pp. 155–169 (1961).

[14] R. F. Hills, B. W. Howlett, B. R. Butcher, "Further studies on the decomposition of the γ phase in uranium-low molybdenum alloys," *J. Less Common Metals*, 5:5, pp. 369–373 (1963).

[15] B. W. Howlett, A. J. Eycott, I. K. Kang, D. R. F. West, "The kinetics of the isothermal decomposition of a gamma-phase uranium - 6 atomic % molybdenum alloy," *J. Nucl. Mate.s*, 9:2, pp. 143–154 (1963).

[16] G. Östberg, M. Möller, B. Schönntng-Christiansson, "Metallographic study of the transformation of γ phase into (α + γ') phases in a U-1.6 wt% Mo alloy," *J. Nucl. Mater*., 10:4, pp. 329–338 (1963).

[17] P. E. Repas, R. H. Goodenow, and R. F. Hehemann, "Transformation Characteristics of U-Mo and U- Mo-Ti Alloys," *Trans. Am. Soc. Metals*, 13:1 (1964) pp. 150-63

[18] G. Östberg, B. Lehtinen, "The α+γ' ordering reaction during isothermal transformation of γ in a U-1.6 wt% Mo alloy," *J. Nucl. Mater*., 13:1 (1964) pp. 123–124

[19] Y. Goldstein and A. Bar-Or, *J. Inst. Met*., Vol. 95, (1967) pp. 17-21

[20] C. W. Tucker, "Discussion on the Constitution of Alloys by C. L. Pfeil in the Journal Journal of the Institute of Metals, 77: pp. 553-570 (1950)," Report AECD-3092, United States Atomic Energy Commission (1951).
[21] H. A. Saller, F. A. Rough, and D. A. Vaughan, "The Constitution Diagram of Uranium-Rich Uranium-Molybdenum Alloys," report BMI-72, United States Atomic Energy Commission (1951).
[22] H. A. Saller, F. A. Rough, and D. C. Bennett, "The Constitution Diagram of Molybdenum-Rich Uranium-Molybdenum Alloys," report BMI-730, U.S. Atomic Energy Commission (1952)
[23] H. A. Saller, and F. A. Rough, "Alloys of Uranium with Zirconium, Chromium, Columbium Vanadium, and Molybdenum," report BMI-752, United States Atomic Energy Commission (1952).
[24] O. S. Ivanov, T. A. Badaeva, R. M. Sofronova, V. B. Kishenevshii, N. P. Kushnir, and O. S. Ivanov, "Phase Diagrams of Uranium Alloys," Amerind Publishing Co. Pvt. Ltd., New Delhi, India (1983).
[25] A. E. Dwight, "The uranium-molybdenum equilibrium diagram below 900° C," *J. Nucl. Mater*., 2, pp. 81–87 (March 1960).
[26] B. W. Howlett, A. J. Eycott, I. K. Kang, D. R. F. West, "The kinetics of the isothermal decomposition of a gamma-phase uranium - 6 atomic % molybdenum alloy," *J. Nucl. Mater*., 9, pp. 143–154 (July1963).
[27] P. E. Repas, R. H. Goodenow, and R F Hehemann, "Transformation Characteristics of U-Mo and U-Mo-Ti Alloys," *Trans. Am. Soc. Metals*, 13, pp. 150-63 (1964).
[28] Y. Goldstein and A. Bar-Or," DecompositionKinetics of Gamma Phase Uranium Alloys Containing 8, 10.8, and 14.3 wt% Molybdenum," *J. Inst. Met*., 95, pp. 17-21 (1967).
[29] R. J. Van Thyne, D. J. McPherson, "Transformation Kinetics of Uranium-Molybdenum Alloys," *Trans. ASM* 49, pp. 598-621 (1957).
[30] R. J. Van Thyne, *Uranium Alloys Newsletter*, 13 (1955).
[31] G. Cabane, G. Donzé, "Stabilisation de la Phase γ dans les Alliages Ternaires à Base D'Uranium-Molybdene," *J. Nuc. Mat*., 4, pp. 364-73 (1959).
[32] F. Giraud-Heaud, J. Guillaumin, "Formationde Phases de Transition Dans L'Alliage U-7.5Nb-2.5Zr," *Acta. Met*. **21** 1243-52 (1973)
[33] D. A. Lopes, T. A. G. Restivo, A. F. Padilha, *J. Nucl. Mater*., 440, pp. 304–309 (2013).
[34] C. A. W. Peterson, R. R. Vandervoot, The Properties of a Metastable Gamma-phase Uranium Based Alloy: U–7.5Nb –2.5Zr, Lawrence Radiation Laboratory report UCRL-7869, University of California, Livemore (1964).
[35] R. M. Willard and A. R. Schmitt, "Irradiation Swelling, Phase Reversion and Intergranular Cracking of U-10wt%Mo Fuel Alloy", Atomics International report NAA-SR-8956 (1964).
[36] A. A. Shoudy, W. E. McHugh and M. A. Silliman, "The Effect of Irradiation Temperature and Fission Rate on the Radiation Stability of Uranium-10 wt% Molybdenum Alloy," Radiation Damage in Reactor Materials, pp. 133-162 (1963).
[37] M. K. Meyer, G. L. Hofman, S. L. Hayes, C. R. Clark, T. C. Wiencek, J. L. Snelgrove, R. V. Strain, K-H Kim, "Low-temperature irradiation behavior of uranium- molybdenum alloy dispersion fuels," *J. Nucl. Mater*., 304, pp. 221-236 (2002).
[38] A. Leenaers, S. Van den Berghe, E. Koonen, C. Jarousse, F. Huet, M. Trotabas, M. Boyard, S. Guillot, L. Sannen, M. Verwerft, *J. Nucl. Mater*., 335, pp 39-47 (2004).
[39] P. Lemoine, D. M. Wachs, Proceedings of the International Conference on Research Reactors: Safe Management and Effective Utilization Sydney, Australia, (2007).
[40] F. Huet, J. Noirot, V. Marelle, S. Dubois, P. Boulcourt, P. Sacristan, S. Naury, P. Lemoine, "Post Irradiation Examinations on UMo Full Sized Plate – IRIS2 Experiment," Transactions of the 9th International Topical Meeting on Research Reactor Fuel Management, Budapest, Hungary (2005).
[41] S.Van den Berghe, U. Parthoens, G. Cornelis, S. Leenaers E.Koonen, V. Kuzminov, C. Detavernier, "*Swelling of U(Mo) dispersion fuel under irradiation-Non-destructive analyses of the SELNIUM plates*" Journal of Nuclear Materials 442 (2013) 60-68.
[42] D. D. Keiser Jr., J-F Jue, A.B. Robinson, P. Medvedev, J. Gan, B.D. Miller, D.M. Wachs, G.A. Moore, C.R. Clark, M.K. Meyer, M.R. Finlay, "Effects of Irradiation on the Microstructure of U-7Mo Dispersion Fuel with Al-2Si Matrix," *J. Nucl. Mater*., 425 pp. 156-172 (2012).
[43] D. D. Keiser Jr, D.M. Wachs, M.K. Meyer, A.B. Robinson, P. Medvedev, G.A. Moore, "Microstructural Analysis of Irradiated U-Mo Fuel Plates: Recent Results," Transactions of the 16th International Topical Meeting on Research Reactor Fuel Management, Prague, Czech Republic, March 18-22, (2012).
[44] G. L. Hofman and M. K. Meyer, "Progress in Irradiation Performance of Experimental Uranium- Molybdenum Dispersion Fuel", Proceedings of the International Meeting on Reduced Enrichment for Research and Test Reactors, Bariloche, Argentina, November 3-8 (2002).
[45] I. G. Prokofiev, T. C. Wiencek, B. D. Merkle, E. O. Carney, "Monolithic Fuel Plates Diffusion Bonded by Electroconsolidation® Process Technology", Proceedings of the International Meeting on Reduced Enrichment for Research and Test Reactors, Boston, Massachusetts, USA, November 6-10 (2005).
[46] C. Jarousse, P. Lemoine, P. Boulcourt , A. Röhrmoser, and W. Petry, "Monolithic UMo Full Size Prototype Plates for IRIS V Irradiation," Transactions of the 11th International Topical Meeting on Research Reactor Fuel Management, Lyon, France, March 11-15 (2007).
[47] D. E. Burkes, D. E, N. P. Hallinan, K. L. Shropshire, P. B. Wells, "Effects on Applied Load on 6061-T6 Aluminum Joined Employing a Novel Friction Bonding Process," *Metal. Mater. Trans*., 39, pp. 2852-2861 (2008).
[48] J. F.Jue, etal, "Fabrication of Monlithic RERTR Fuels by Hot Isostatic Pressing;" Journal of Nuclear Technology, vol 72, No,2, pg.204 210, Nov 2010
[49] G. A. Moore, M.C. Marshall, "Co-rolled U-10Mo/Zirconium *Barrier-Layer Monolithic Fuel Foil Fabrication Process*," Idaho National Laboratory report INL/EXT-10-17774 (2010).
[50] J. F. Jue, D. D. Keiser, C. R. Breckenridge, G. A. Moore, M. K. Meyer, "Microstructural Characteristics of HIP-bonded Monolithic Nuclear Fuels with a Diffusion Barrier," *J. Nucl. Mater*., 448, pp. 250-258 (2014).
[51] A. B. Robinison and M. R. Finlay, "RERTR-7 Post Irradiation Examination (PIE) Letter Report," Idaho National Laboratory,

Idaho National Laboratory report INL/EXT-07-13271 (2007).
[52] D. D. Keiser Jr., A. B. Robinson, J.-F. Jue, P. Medvedev, D. M. Wachs, M. R. Finlay, "Microstructural development in irradiated U-7Mo/6061 Al alloy matrix dispersion fuel," *J. Nucl. Mater*., 393, pp. 311-320 (2009).
[53] A. Leenaers, S. Van den Berghe, J. Van Eyken, E. Koonen, F. Charollais, P. Lemoine, Y. Calzavara, H. Guyon , C. Jarousse, D. Geslin, D. Wachs, D. Keiser, A. Robinson, G. Hofman, Y. S. Kim, "Microstructural evolution of U(Mo) –Al(Si) dispersion fuel under irradiation – Destructive analyses of the LEONIDAS E-FUTURE plates," *J. Nucl. Mater*., 441, pp. 439-448 (2013).
[54] D. L. Porter, "Zry Clad Experiment Report," Idaho National Laboratory report INL/EXT-12-27273 (2012).
[55] O. A. Golosov, S. A. Averin, M. S. Lyutnikov, et al, "Electron-microscopic studies of barrier coatings on U–Mo fuel irradiation to 60% burnup," *Atomic Energy*, 110, pp. 486–494
[56] O. S. Ivanov, G. N. Bagrov, "Isothermal cross sections of the triple system uranium-molybdenum-zirconium at 1000 °C -625 °C.," Struct. Alloys Certain Systems Cont. Uranium Thorium 1963:131
[57] O. S. Ivanov, G. N. Bagrov. "Isothermal cross sections at 600 °C, 575 °C, and 500°C, polythermal sections, and the phase diagram of the triple system Uranium molybdenum-zirconium." *Struct. Alloys*, Certain Systems Cont. Uranium Thorium 1963:154
[58] K. Huang, Y. Park, D. Keiser, and Y. Sohn, "Interdiffusion Between Zr Diffusion Barrier and U-Mo Alloy," *J. Phase Equil. Diffus*., 33, pp. 443-449 (2013).
[59] E. Perez, B. Yao, D. D. Keiser Jr, and Y. H. Sohn, "Microstructural analysis of as processed U-10 wt.% Mo monolithic fuel plate in AA6061 matrix with Zr diffusion barrier," *J. Nucl. Mater*., 402, pp. 8-14 (2010).
[60] G. V. Kidson, G. D. Miller, "A study of the interdiffusion of aluminum and zirconium," *J. Nucl. Mater*., 12, pp. 61-69 (1964).
[61] A. Laik, K. Bhanumurthy, G. B. Kale, "Intermetallics in the Zr–Al diffusion zone," *Intermetallics*, 12, pp. 69-74 (2004).
[62] J. Dickson, L. Zhou, A. Ewh, M. Fu, D. Keiser, Jr., and Y. Sohn "Interdiffusion and Reaction between Zr and Al Alloys from 450 to 625˚C," *Intermetallics*, 49 pp. 154-162 (2014).
[63] G. L. Hofman, L .C. Walters, T. H. Bauer, "Metallic Fast Reactor Fuels," *Prog. Nucl. Ener*., 31, pp. 83-110 (1997).
[64] J. Gan, D. D. Keiser, B. D. Miller, A. B. Robinson, J. F. Jue, P. Medvedev, D. M. Wachs, "TEM Characterization of U-7Mo/Al-2Si Dispersion Fuel Irradiated to Intermediate and High Fission Densities," *J. Nucl. Mater*., 424, pp. 43-50 (2012).
[65] J. S. Van den Berhe, W. Van Renterghem, A. Leenaers, "Transmission Electron Microscopy Investigation of Irradiated U-7wt.% Mo Dispersion Fuel," *J. Nucl. Mater*., 375, pp. 340-346 (2008).
[66] J. Rest, "Evolution of fission-gas-bubble-size distribution in recrystallized U-10Mo nuclear fuel," *J. Nucl. Mater*., 407 pp. 55-58 (2010).
[67] Y. S. Kim, G. L. Hofman, J. S. Cheon, "Recrystallization and swelling of U-Mo fuel during irradiation," Transactions of the 16th International Topical Meeting on Research Reactor Fuel Management, Prague, Czech Republic, March 18-22, (2012).
[68] Y. S. Kim, G. L. Hofman, "Fission Product Induced Swelling of U-Mo Alloy Fuel", *J. Nucl. Mater*., 419, pp. 291-301 (2011).
[69] D. Keiser, Jr., et al., "SEM Characterization of the High Burn-up Microstructure of U-7Mo Alloy", Transactions of the 18th International Topical Meeting on Research Reactor Fuel Management, Ljubljana, Slovenia, March 30-April 3 (2014).
[70] J. Gan, et al., "TEM Characterization of High Burn-up Microstructure of U-7Mo Alloy", Transactions of the 18th International Topical Meeting on Research Reactor Fuel Management, Ljubljana, Slovenia, March 30-April 3 (2014).
[71] Y. S. Kim, G. L. Hofman, J. S. Cheon, A. B. Robinson, and D. M. Wachs "Fission Induced Swelling and Creep in Uranium Molybdenum Alloy Fuel," *J. Nucl. Mater*., 437, pp. 37-46 (2013).
[72] A. Leenaers, et. al., "Microstructure of U3Si2 Fuel Plates Submitted to a High Heat Flux," *J. Nucl. Mater*., 327, pp. 121-129 (2004).
[73] Z. Hashin and S. Shtrikman, "A Variational Approach to the Theory of the Effective Magnetic Permeability of Multiphase Materials," *J. Applied Physics*, 33, pp. 3125-3131 (1962).